

REPORT DOCUMENTATION PAGE

Form Approved
OMB No. 0704-01-0188

The public reporting burden for this collection of information is estimated to average 1 hour per response, including the time for reviewing instructions, searching existing data sources, gathering and maintaining the data needed, and completing and reviewing the collection of information. Send comments regarding this burden estimate or any other aspect of this collection of information, including suggestions for reducing the burden to Department of Defense, Washington Headquarters Services, Directorate for Information Operations and Reports (0704-0188), 1215 Jefferson Davis Highway, Suite 1204, Arlington VA 22202-4302. Respondents should be aware that notwithstanding any other provision of law, no person shall be subject to any penalty for failing to comply with a collection of information if it does not display a currently valid OMB control number.

PLEASE DO NOT RETURN YOUR FORM TO THE ABOVE ADDRESS.

1. REPORT DATE (DD-MM-YYYY) 08-04-2005		2. REPORT TYPE REPRINT		3. DATES COVERED (From - To)	
4. TITLE AND SUBTITLE Ion Scattering in a Self-consistent Cylindrical Plasma Sheath				5a. CONTRACT NUMBER	
				5b. GRANT NUMBER	
				5c. PROGRAM ELEMENT NUMBER 61102F	
6. AUTHORS Shana S. Figueroa, D.L. Cooke, and Nikos A. Gatsonis*				5d. PROJECT NUMBER 5021	
				5e. TASK NUMBER RS	
				5f. WORK UNIT NUMBER A1	
7. PERFORMING ORGANIZATION NAME(S) AND ADDRESS(ES) Air Force Research Laboratory / VSBXT 29 Randolph Road Hanscom AFB, MA 01731-3010				8. PERFORMING ORGANIZATION REPORT NUMBER AFRL-VS-HA-TR-2007-1095	
9. SPONSORING/MONITORING AGENCY NAME(S) AND ADDRESS(ES)				10. SPONSOR/MONITOR'S ACRONYM(S) AFRL/VSBXT	
				11. SPONSOR/MONITOR'S REPORT NUMBER(S)	
12. DISTRIBUTION/AVAILABILITY STATEMENT Approved for Public Release; distribution unlimited.					
13. SUPPLEMENTARY NOTES Reprinted from Proceedings, 9 th Spacecraft Charging Technology Conference, Tsukuba, Japan, 4-8 April 2005. *Worcester Polytechnic Institute, Worcester, MA 01609					
14. ABSTRACT Results are presented from a study of charged particle scattering about a charged wire in an ionospheric plasma. The one dimensional case assumes an infinite wire in an unmagnetized plasma with finite and equal ion and electron temperatures. Because particle energy and angular momentum are conserved in such a formulation, the results have the potential to provide a standard against which to compare more complicated electrodynamic tether simulations. Results indicate that higher plasma shielding limits the range of impact parameters that experience significant scattering, and that attracted particles entering tangent to the sheath experience increased scattering. The results also show that there are significant changes in orbital trajectories between different space charges within the OML limit.					
15. SUBJECT TERMS Spacecraft charging Plasma simulation, Nascap-2k					
16. SECURITY CLASSIFICATION OF:			17. LIMITATION OF ABSTRACT	18. NUMBER OF PAGES	19a. NAME OF RESPONSIBLE PERSON
a. REPORT	b. ABSTRACT	c. THIS PAGE			Adrian Wheelock
UNCL	UNCL	UNCL			19b. TELEPHONE NUMBER (Include area code)

Ion scattering in a Self-consistent Cylindrical Plasma Sheath

Shana S. Figueroa and David L. Cooke

Air Force Research Laboratory, Space Vehicles Directorate, Hanscom AFB, MA 01731

Nikos A. Gatsonis

*Mechanical Engineering Department, Worcester Polytechnic Institute, Worcester, MA 01609***Abstract**

Results are presented from a study of charged particle scattering about a charged wire in an ionospheric plasma. The one dimensional case assumes an infinite wire in an unmagnetized plasma with finite and equal ion and electron temperatures. Because particle energy and angular momentum are conserved in such a formulation, the results have the potential to provide a standard against which to compare more complicated electrodynamic tether simulations. Results indicate that higher plasma shielding limits the range of impact parameters that experience significant scattering, and that attracted particles entering tangent to the sheath experience increased scattering. The results also show that there are significant changes in orbital trajectories between different space charges within the OML limit.

1. Introduction

Current plasma models employ complicated codes for analyzing plasma characteristics as realistically as possible, taking into account many factors such as particle collisions, multiple sheaths, trapped particles, interacting magnetic fields, etc. As a result of so many variables, a new model needs to be tested against a standard or "classical" theory to verify the results. Of course comparison with experiment is the ultimate validation, but in many cases and end to end comparison does not provide as much insight into phenomenon and errors as code to code verification. Generally, a suitable classical model is one that involves minimal assumptions, many conserved quantities, a high degree of analyticity, and of course community acceptance.

This paper seeks to provide a classical plasma sheath model for particle scattering for the case of an infinitely long charged wire immersed in an unmagnetized plasma with finite plasma temperature. Under these conditions, charged particles will orbit the wire conserving both energy and angular momentum. This allows us to compute the self-consistent space charge sheath using the Turning Point Method [1], and then numerically compute the scattering of particles in the electric field of the wire. Although the scattering must be computed numerically for the general case, the conserved elements of the orbit allow this to be done in semi-analytic one dimensional integral. In the case of a r^{-1} potential we can compare our results to the fully analytic answer.

The Turning Point Method, or TPM, was developed by Parker [1] and provides a self-consistent solution when calculating the characteristics of a collisionless, isotropic and stationary plasma in the presence of a probe with a large radius compared to the plasma debye length. Using the TPM to analyze a plasma provides an advantage over other plasma theories in several ways. By being able to identify the point where a particle turns in its orbit, the entire trajectory of the particle can be traced to and from infinity without having to know any other information about the particle's orbit. This provides a

20071002164

DTIC COPY

much simpler alternative to the computationally intensive particle-in-cell (PIC) weighting method, which must perform individual calculations along the entire trajectory of the particle. The TPM is also easier to develop into a computer program than Laframboise's earlier Effective Potential Method [2], which is equivalent to the TPM. The TPM also provides a straightforward method for determining the turning angle of a particle along its orbit.

This paper will specifically look at the case of a charged particle either attracted or repelled to a charged cylindrical probe by using a Fortran code originally developed by Cooke [3]. The original program, called TurningPoint, used Fortran 77 to model the characteristics of a particle that could either be attracted to or repelled by a spherical probe using the TPM. In this effort, the code was expanded to include the analysis of a plasma using cylindrical probe geometry, as well as an added subroutine that finds the turning angle of the charged particle (repelled or attracted) around the probe.

2. Background

The goal of a probe theory is to determine the charge density, particle flux, and the electrical potential about the probe. To find the current density and potential, two governing equations are used – the Vlasov equation and Poisson's equation. Poisson's equation states

$$\nabla \Phi^2 = -\rho / \epsilon_0 \quad ; \quad \Phi = \frac{e\phi}{kT} \quad , \quad \rho = e(n_i - n_e) \quad (1)$$

where Φ is the plasma potential, ρ is the net particle density, ϵ_0 is the permittivity of space, e is the particle charge, ϕ is the particle voltage, k is the Boltzmann constant, T is the particle temperature, n_i is the ion density and n_e is the electron density. The time-independent form of Vlasov's equation is given as

$$\vec{V} \cdot \nabla_r f + \frac{e}{m} \nabla_r \Phi \cdot \nabla_v f = 0 \quad (2)$$

where ∇_r and ∇_v denote the gradient operator with respect to position and velocity space, and f and m are the velocity distribution and the mass of the particle, respectively. In this analysis we assume the velocity distribution, f , to be Maxwellian for both electrons and ions. With the proper boundary conditions, it is possible to manipulate Vlasov's equation in order to solve for the particle density, known as the "Vlasov Problem"; conversely, Poisson's equation can be solved to yield the electrical potential given a constant particle density, known as the "Poisson Problem". By solving the Vlasov Problem and the Poisson Problem simultaneously on a set of grid points, the particle (and therefore current) density and the plasma potential can be determined.

2.1. The Vlasov Problem

Solving the Vlasov Problem requires solving the Vlasov equation for a set of boundary conditions that classifies the particle orbits into whether or not they contribute to the current density measured by the probe. The current density is defined as the first moment of the Vlasov equation:

$$I(\vec{R}) = \iiint f(\vec{R}, \vec{V}) V_n d^p \vec{V} \quad (3)$$

where p is 2 for a cylindrical probe and 3 for a spherical probe. Assuming a Maxwellian velocity distribution, expressing the current density for a cylindrical probe in a dimensionless form, i , yields

$$i = \frac{4}{\sqrt{\pi}} \int_{v_{\min}}^{\infty} \exp(-v^2 - \phi) v^2 dv \int d(\sin \theta). \quad (4)$$

Here, ϕ and v are dimensionless quantity defined as $\phi = \Phi(kT/e)$ and $v = V/(2kT/m)^{1/2}$. The evaluation of the current density can be simplified by transforming the integration of n over v and θ into integration over the constants of motion, E and J^2 , where E is the total energy of the particle and J^2 is the square of the angular momentum. Using E and J^2 is advantageous because these variables remain constant throughout the entirety of the particle's orbit, regardless of changes in r along that orbit. The constants of motion in dimensionless form are

$$E = v^2 + \phi \quad ; \quad J^2 = r^2 v^2 \sin^2 \theta \quad (5)$$

Transformation of the current density using E and J^2 yields

$$i = \frac{2}{\sqrt{\pi}} \exp(\phi_{\text{source}}) \int_{v_{\min}}^{\infty} \exp(-E) dE \cdot M_{ic}(E). \quad (6)$$

ϕ_{source} is the potential at the source, which is ϕ_{∞} for ambient particles and zero otherwise [4]. M_{ic} is the "monoenergetic" contribution to i for a cylindrical probe, defined as

$$M_{ic}(E) = \int \delta \cdot d \left(J^2 / r^2 \right)^{1/2} \quad (7)$$

where E is held constant and the integrals are evaluated over J^2 . The factor C represents a differentiation between ambient and emitted particles, where C is unity for ambient particles and 2 for emitted particles. The factor δ gives orbit information pertaining to what source an orbit will connect with. Thus, for ambient particles, $\delta=1$ if the particle comes from infinity and $\delta=0$ if it comes from the probe surface. Similarly, for emitted particles $\delta=0$ if the particle comes from infinity and $\delta=1$ if it comes from the surface. Simply put, a nonzero value for δ means that an orbit is "occupied". Evaluating M_{ic} requires that the boundary conditions for the integral be determined, which can be done by defining specifically which particles have an angular momentum that contribute to the collected probe current and which do not. This is where the TPM becomes useful.

The TPM defines a turning point as the point where the radial velocity component $v_r = 0$. Consequently, a particle will not vanish or change sign (i.e. a particle will exist) as long as

$$E > \phi + \frac{J^2}{r^2} \quad (8)$$

or

$$J^2 < g \equiv r^2 (E - \phi) \quad (9)$$

In the above equation, g is defined as the turning-point function. When g is plotted in the (J^2, r) plane, all physically possible orbits exit below the turning-point function curve.

In a collisionless plasma, there are four types of orbits can exist (illustrated in Figure 1):

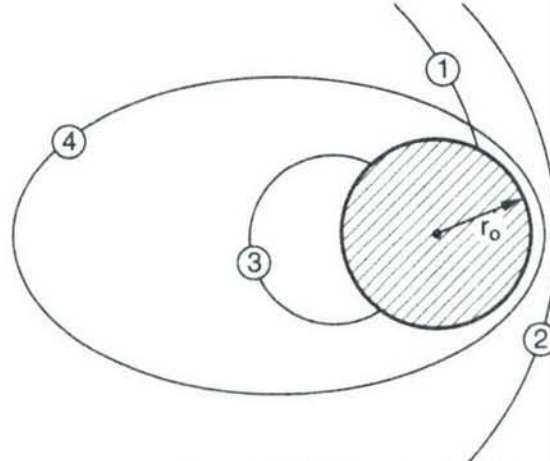


Figure 1: The 4 types of orbits

Type 1: Orbits that include ambient particles that pass from infinity to the sphere, or emitted particles that pass from the sphere to infinity. These orbits have no turning point and $\delta = 1$.

Type 2: Orbits that include ambient particles that pass from infinity by the probe at a minimum radius without intersecting the probe surface, and back out to infinity again. These particles have one turning point and a delta factor of $\delta = 2$ to account for the ingoing and outgoing trajectory contributions of the particle.

Type 3: Orbits that comprise of particles emitted from the surface of the probe that travel out to a maximum radius and then return back to the probe surface. Particles in type 3 orbits have one turning point and a delta factor of $\delta = 2$ to account for the ingoing and outgoing trajectory of the particle.

Type 4: Closed or “trapped” orbits where particles circle the probe indefinitely without making contact with the surface. These orbits are assumed to be unpopulated in collisionless plasmas and therefore $\delta = 0$ for them.

From analysis of the orbit types, it is evident that type-1 and type-2 orbits can contribute to the collected probe current simultaneously, and type-1 and type-3 orbits can contribute simultaneously, but type-2 and type-3 orbits cannot contribute simultaneously. Also, there will always be contributions by type-1 orbits between the lowest value of J^2 and $J^2 = 0$. Hence, there can be orbits populated by either type-2 or type-3 orbits above the minimum J^2 .

When the turning-point function, g , is plotted in the (J^2, r) plane, the least-values of g can be analyzed in relation to the radial position, r , at where they occur. Here, three cases are considered that encompass the relevant scenarios: case A - the least value of $g(r)$ (known as the “absorption radius”) occurs inside of the probe radius, r_p , case B – the least value of $g(r)$ occurs outside of r_p , and case C – there is a least value of $g(r)$ inside of r_p and a secondary least-value outside of r_p . The three cases are illustrated in Figure 2.

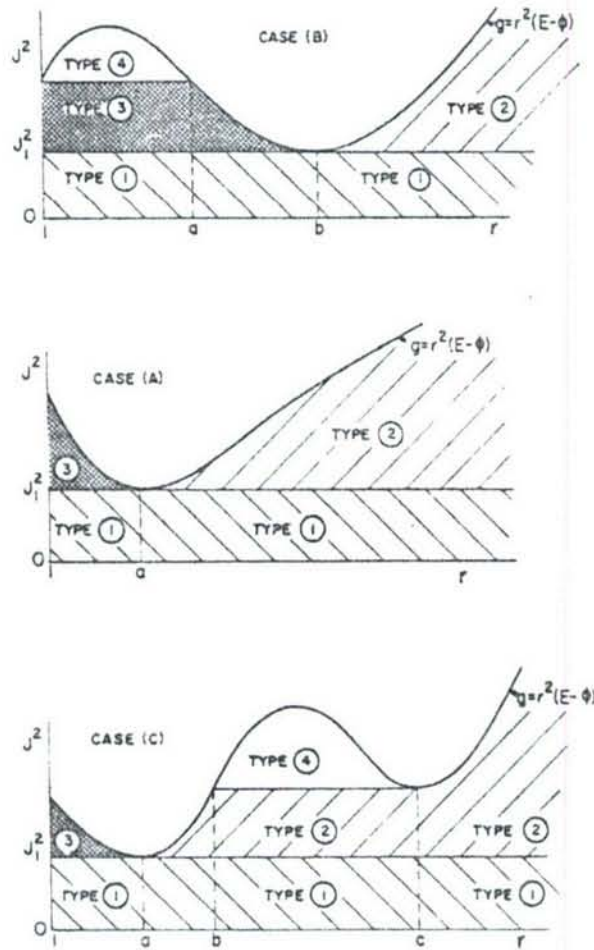


Figure 2: Case A,B and C in (r, J^2) space

In case A, the least value of g occurs at point a , and corresponds to the least value of $J^2 = J_l^2$. Only type-1 orbits exist between $J^2 = 0$ and $J^2 = J_l^2$ and, since type-2 orbits are outside of the absorption radius and type-3 orbits are inside the absorption radius, we have

Case A: For $r(1,a)$, $J_{A1}^2 = 0$, $J_{B1}^2 = J_{A3}^2 = J_l^2$, $J_{B3}^2 = g(r) \rightarrow$ no type-2 orbits

For $r(a,\infty)$, $J_{A1}^2 = 0$, $J_{A2}^2 = J_l^2$, $J_{B2}^2 = g(r) \rightarrow$ no type-3 orbits

Case A is the only case that we will analyze for the purposes of this paper. From this analysis, it is possible to define M_{ic} for ambient or surface-emitted particles for a cylindrical probe. The analysis is done in Parker [4] with the results as follows:

$$M_{ic}(E) = \int_0^{\sqrt{E-\phi}} \delta \cdot d \left(J^2 / r^2 \right)^{1/2} = \left(J_l^2 / r^2 \right)^{1/2} = J_l \quad (10)$$

In this case, $r = 1$ since the current density of interest is that collected at the probe surface.

To finish solving the Vlasov Problem, the integral over energy in equation (6), with M_{ic} defined in equation (10), must be numerically evaluated using a quadrature formula in the form

$$\int_{E_{min}}^{\infty} \exp(-E) dE \cdot M(E) = \sum_{k=1}^K C_k \cdot M(E_k) \quad (11)$$

where C_k is a constant that varies with the energy E_k from $k = 1, 2, \dots, K$. C_k and E_k are evaluated by establishing a least value and greatest value of the potential distribution, E_{min} and E_{max} . The integral can now be split up into two parts, one in the finite range of (E_{min}, E_{max}) and one in the semi-infinite range of (E_{max}, ∞) :

$$\int_{E_{min}}^{\infty} \exp(-E) dE \cdot M(E) = \int_{E_{min}}^{E_{max}} \exp(-E) dE \cdot M(E) + \int_{E_{max}}^{\infty} \exp(-E) dE \cdot M(E) \quad (12)$$

The finite range consists of type-3 and type-4 orbits, where the potential dips into the negative range along the orbit as the particle changes trajectory around the probe. Consequently, when only considering type-1 and type-2 orbits (or only case A scenarios), $E_{min} = E_{max}$ and only the semi-infinite range applies.

For the Maxwellian case where the integrand contains a Gaussian function as a weighted function, the coefficients C_k and E_k can be transformed into an abscissa-coefficient pair defined from the data of Steen et al., and the semi-infinite range integral becomes

$$\int_{E_{max}}^{\infty} \exp(-E) dE \cdot M(E) = \exp(-E_{max}) \int_0^{\infty} \exp(-U) dU \cdot M(U + E_{max})$$

$$= \sum_{k=1}^K 2H_k a_k \cdot M(a_k^2 + E_{\max}) \quad (13)$$

Here, $C_k = 2H_k a_k$ and $E_k = a_k^2 + E_{\max}$, where H_k and a_k are the abscissa-coefficient pair defined in Steen et al.

This completes the solution to the Vlasov Problem. Next, the much simpler Poisson Problem will be solved.

2.2. The Poisson Problem

Poisson's equation, given earlier as equation (1), can be rewritten in dimensionless form using the dimensionless terms described earlier plus λ_d , which is the ambient-electron Debye length, λ_D , divided by r_0 (the "Debye number"). For a cylinder, Poisson's equation may be transformed to

$$\frac{d^2 \phi}{du^2} = \frac{e^{2u}}{\lambda_d^2} (n_e - n_i) \quad (14)$$

In the cylindrical case, $u = \ln r$. Through the transformation of Poisson's equation, it is possible to solve for the electrical potential and obtain a result that is easily analyzed through computational means:

$$\phi_{j-1} - 2\phi_j + \phi_{j+1} = (\Delta u)^2 \left[\frac{e^{2u}}{\lambda_d^2} (n_e - n_i) \right]_j. \quad (15)$$

Δr and Δu are the interval lengths on a uniform grid, and i and j denote the grid point of immediate analysis.

2.3. Turning Angle Calculations

It is desirable to express the equation of the orbit of a particle in terms of r and θ while eliminating the time dependence, with E and J as constants of integration. In a central force problem (where the only two forces interacting with each other are the particle and the probe), the orbit is symmetrical about the turning points, meaning that if any two turning points are known, the complete orbit of the particle can be traced [5]. The classical equation of motion for angular momentum states that

$$l = mr^2 \dot{\theta} \quad (16)$$

where l is the angular momentum with dimensions. Equation (16) can be rewritten as

$$d\theta = \frac{l dt}{mr^2}. \quad (17)$$

Since conservation of energy states that

$$E = \frac{1}{2} m(\dot{r}^2 + r^2 \dot{\theta}^2) + V(r) \quad (18)$$

and assuming that E is a constant of motion, we can solve for dt and combining it with $d\theta$ to eliminate t from the solution for a time-independent result for $d\theta$.

$$d\theta = \frac{ldr}{mr^2 \sqrt{\frac{2}{m} \left(E - V(r) - \frac{l^2}{2mr^2} \right)}} \quad (19)$$

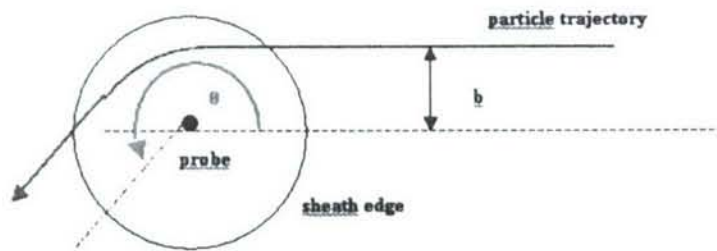
When equation (19) is transformed into units used by Parker and the Turning Point formulation, the result is

$$d\theta = \frac{dr}{r \sqrt{\frac{g(r)}{J^2} - 1}} \quad (20)$$

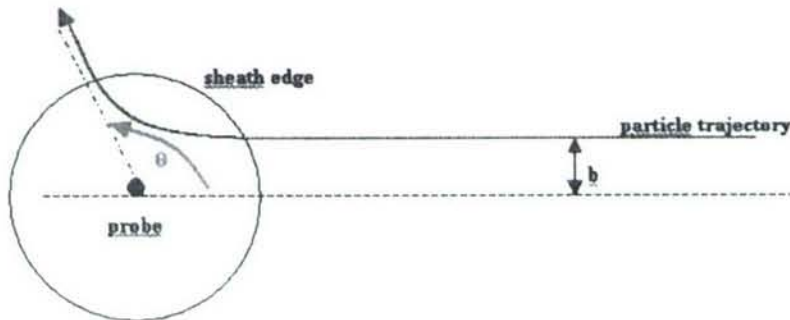
For the specific case when $\phi(R) = \phi_{\text{probe}}/R$, an analytical answer for $d\theta$ is available. In Parker notation, it is

$$d\theta = -a \cos \left(\frac{\frac{2J^2}{r\phi_0} - 1}{\sqrt{1 + \frac{4EJ^2}{\phi_0^2}}} \right) \quad (21)$$

By definition, the TPM identifies the position at which a particle of a certain energy will turn in a potential field. A particle with an angular momentum of J^2 (held constant throughout the particle's orbit) will turn at a radius r when it intersects with the turning function (below the curve), g , and proceed back out to infinity along a trajectory symmetrical to its incoming path. Therefore, the TPM can calculate the turning angle of a particle by computing the $d\theta$ s at each grid point out to infinity (effectively the end of the grid) and adding them together to form one θ value for each g function value. $\Delta\theta$ is interpreted according to the following geometry for attracted and repelled particles:



Attracted Particle Trajectories



Repelled Particle Trajectories

By examining the geometry of the problem it is clear that, for an attracted particle trajectory, the turning angle θ will approach 360° as the impact parameter b decreases, and approach 180° as the impact parameter reaches infinity. The repelled particle trajectories do the opposite – θ approach 0° as b decreases and converges to 180° as b goes to infinity.

3.0. Computational Applications of the Turning Point Formulation

Obtaining a numerical solution for the particle density, current density and electrical potential of a plasma requires simultaneously solving Vlasov's and Poisson's equations through the solution of two sub-problems, the Vlasov Problem and the Poisson Problem. The easiest way to solve the two sub-problems is using an iterative procedure on a computer, consisting of developing a certain amount of radial grid points extending from the surface of the probe to an approximation of infinity, which is what TurningPoint does. At each grid point, the Vlasov Problem is solved to yield the particle density, while the Poisson Problem is solved at the same time to yield the electrical potential to produce mutually consistent solutions. For this paper, the TurningPoint program was expanded to include plasma analysis using a cylindrical probe as well as a spherical probe. Specifically, in-depth analysis was done for cylindrical current collection probes. The program modifications consisted of adding "IF" statements that differentiated between spherical and cylindrical probe collection models based on the initial user input, according to the cylindrical current collection and monoenergetic energy definitions described earlier.

The TurningPoint program was also expanded to calculate the trajectory of the particle in question around either an attracting or repelling probe of cylindrical or spherical geometry by calculating the turning angle of the particle from its turning point out to the end of the grid, or an approximation of infinity. A separate subroutine, called

turn_angle, was added to the end of TurningPoint that numerically calculates the turning angle of the particle at each grid point using the electric potential field of the probe defined earlier in the TurningPoint program.

4.0. Conclusions and Results

Several particle trajectories were defined for different amounts of space charge (or debye length, λ_D), for both attracting and repelling particles in a cylindrical and spherical probe sheath. For a probe voltage held at +100 Volts, the turning angle for various attracted and repelled particles of ± 100 Volts for varying amounts of space charge are shown in Figure 3. As expected, Figure 3 shows the repelled particles coming towards the probe from infinity, where their turning angle is 180° , and being increasingly repelled from the probe as they approach. At a close enough impact parameter, the particles are repelled completely and cannot reach the probe. Figure 5 illustrates that a +10 Volt particle approaching a +100 Volt probe cannot even penetrate the probe sheath until it reaches an impact parameter of $\sim 4 \cdot R_{probe}$, at a probe radius of $\sim 27 \cdot R_{probe}$.

An attracted particle coming into the probe from infinity will fall into the probe and approach 360° . Figures 3 and 5 illustrate an interesting phenomenon as the particle first enters the probe sheath – the deflection angle initially jumps up, suggesting that the particle gains $\Delta\theta$ as it transverses across the contours of the probe sheath and then slopes down as the impact parameter decreases and the particle avoids the sheath irregularities. The effect is more striking as the space charge of the plasma increases and the probe sheath radius decreases.

Figure 4 shows the expected result that at lower space charges (high λ_D), the potential profile approaches a $1/r$ characteristic, while at higher space charges (low λ_D) the potential profile approaches a $\log(r)$ characteristic. This behavior makes it possible to test for consistency of the numerical results by testing the analytical solution for $\Delta\theta$ when the potential profile is forced to be $\phi(r) = \phi_{probe}/R$, equation (21). The results, shown in Figure 7, illustrate what the turning angle of a particle of varying energies in a plasma of high space charge would be in the absence of a sheath. Figure 4 also includes the potential profile of a probe with λ_D/R_{probe} of less than 1.0, the OML limit for a cylindrical probe. It is of interest to note that, even though the probe analysis dealt with space charges within the OML limit, significant changes in orbital trajectories between different space charges were still observed.

Result so far support the common sense expectation that higher plasma shielding (low λ_D/R) limits the range of impact parameters that experience significant scattering. Because the analysis of orbital trajectories does not yield information about the intensity of the incoming particles, a discussion about the total scattering cross-section of the particles is not possible. However, the first moment of the orbital trajectories can be calculated, as $\theta_{moment} = \langle \theta \rangle \cdot r_{sheath}$, providing a somewhat arbitrary number that reflects the quantity of particles that will be deflected to some degree by probe. Table 1 illustrates the

result that higher plasma shielding limits the range of impact parameters that experience significant scattering.

λ_D/R_{probe}	Attracted, θ_{mom} (radians* R/R_{probe})	Repelled, θ_{mom} (radians* R/R_{probe})
1	35.6	40.6
3	144.4	159.9
5	264.6	294.3
10	431.1	510.0
30	571.2	708.5

Table 1: Turning Moment, $V_{probe} = 100V$

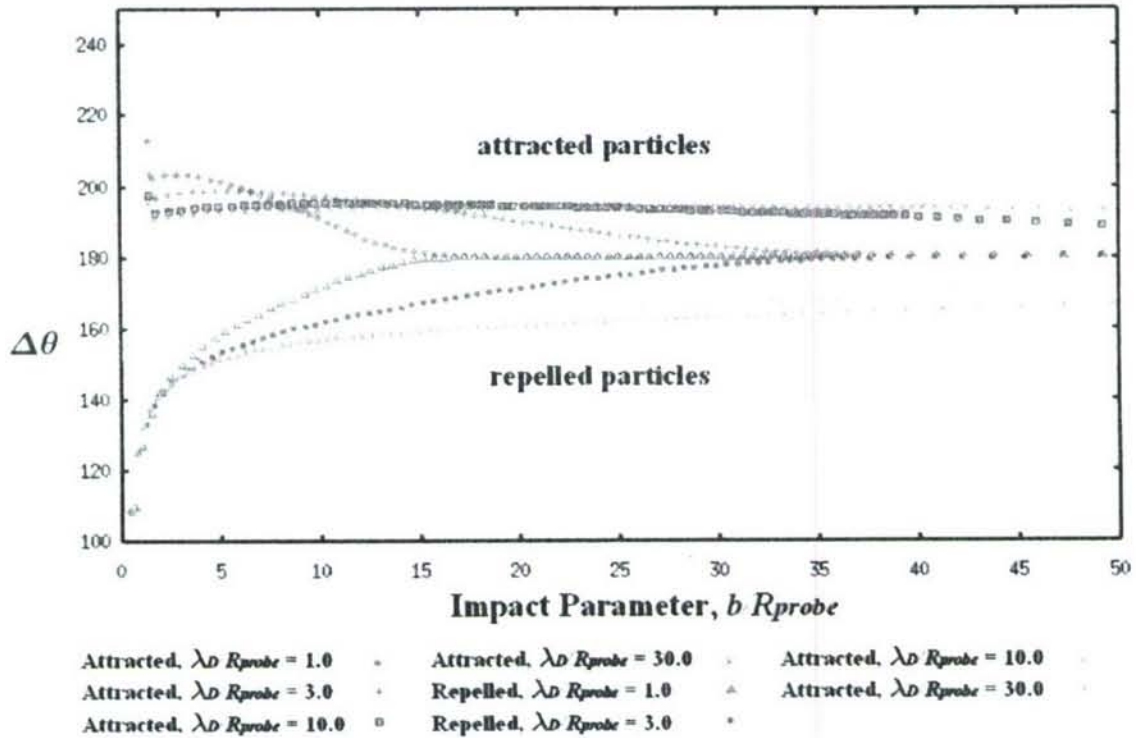


Figure 3: Turning Angle vs Impact Parameter for Attracted and Repelled Particles where $V_{probe} = +100$ Volts and $V_{particle} = \pm 100$ Volts

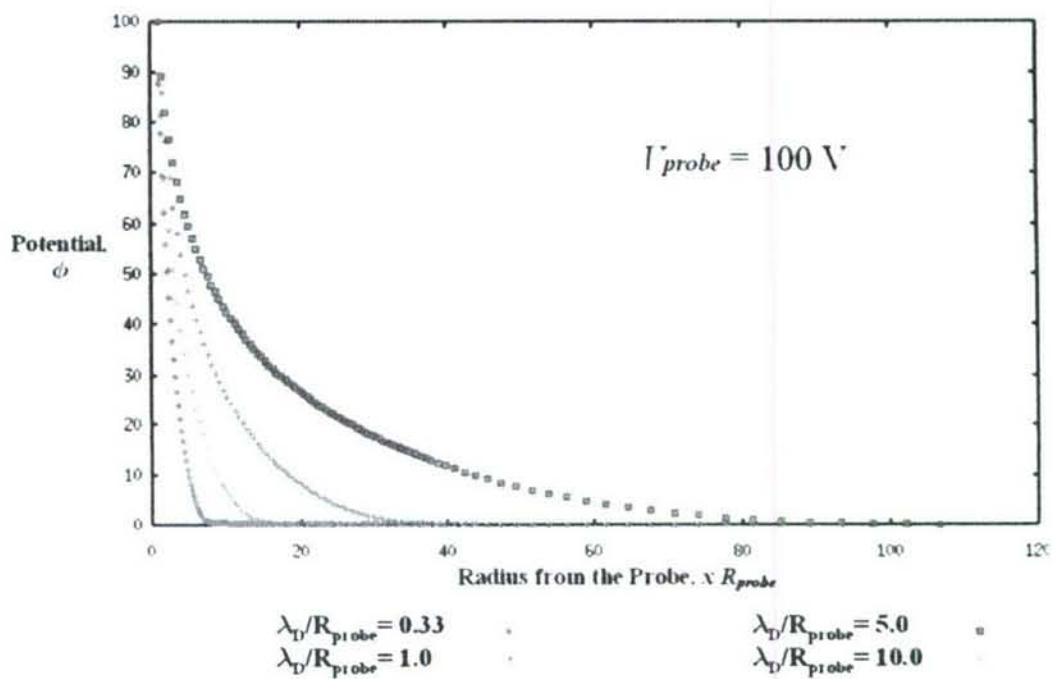


Figure 4: Electric Potential vs Radius from the Probe For Different Debye Lengths

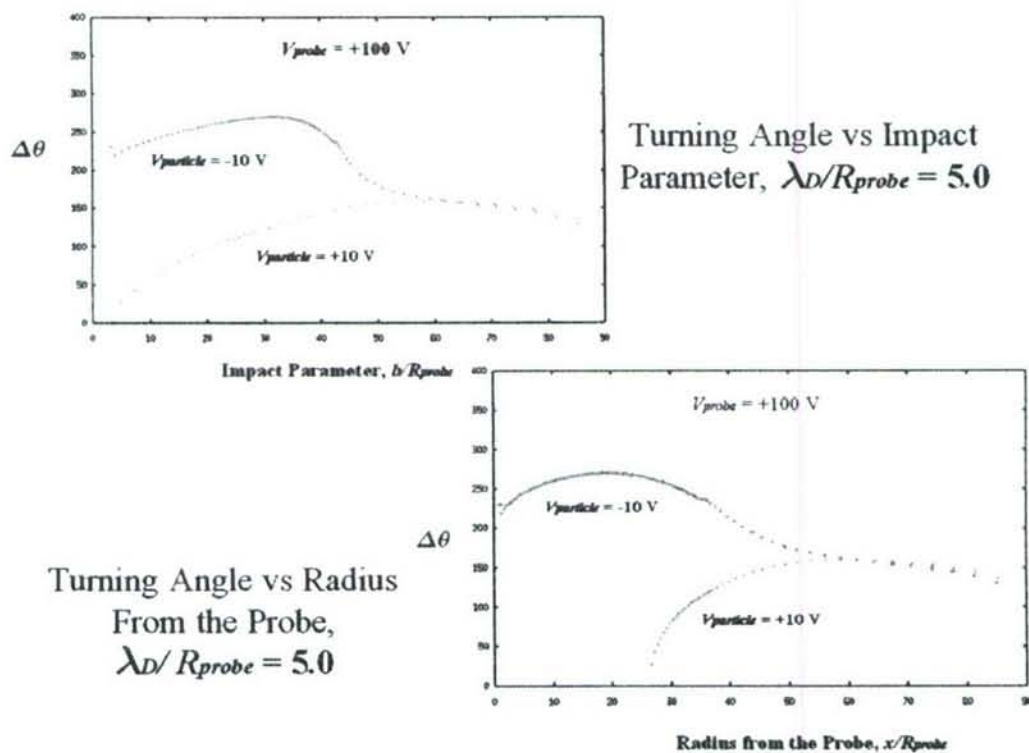


Figure 5: Impact Parameter vs Impact Parameter and Radius from the Probe

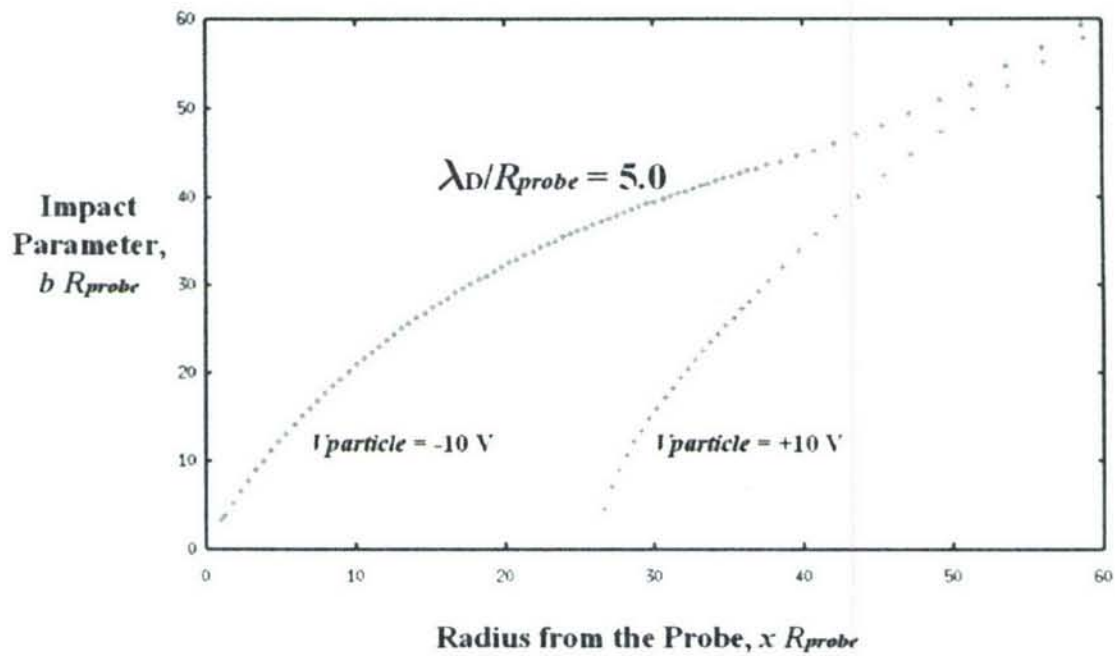


Figure 6: Radius from the Probe vs Impact Parameter for $V_{probe} = +100 \text{ V}$ and $V_{particle} = \pm 10 \text{ V}$

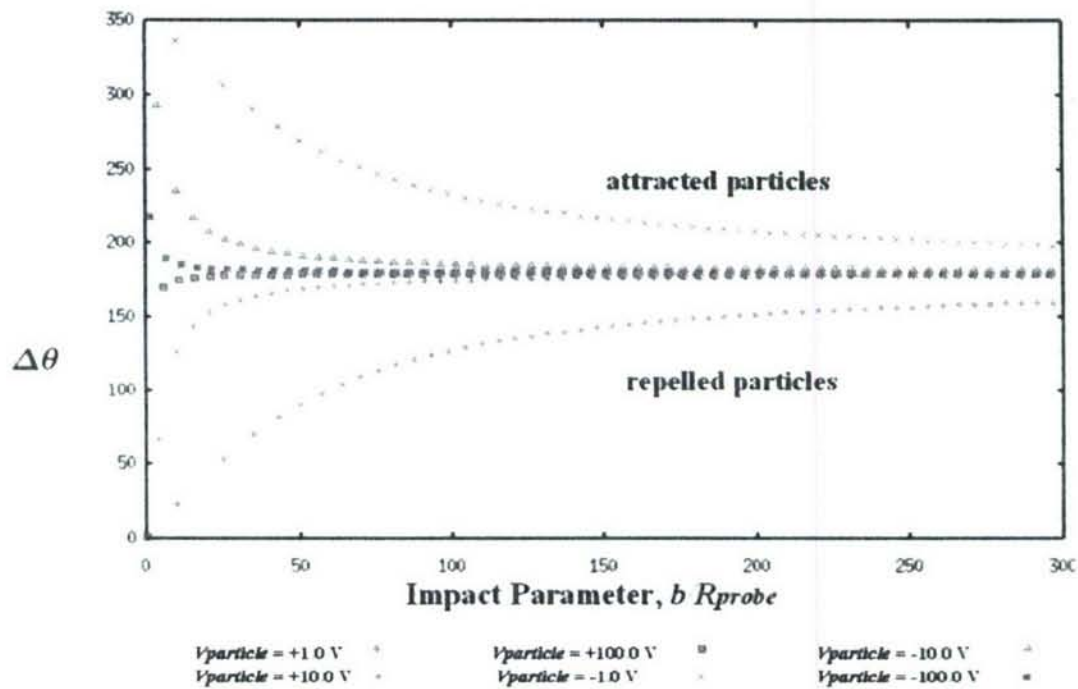


Figure 7: Turning Angle vs Impact Parameter for Attracted and Repelled Particles where $V_{probe} = +100 \text{ Volts}$ for the Case Where $\phi(r) = \phi_{probe}/R$

References

[1] Parker, L.W., "Plasma-Photosheath Theory for Large High-Voltage Space Structures", Space Structures and Their Interactions With Earth's Space Environment, Vol.71, AIAA 1980.

[2] Laframboise, J.G., "Theory of Spherical and Cylindrical Langmuir Probes in a Collisionless Maxwellian Plasma at Rest", University of Toronto Institute of Aerospace Studies, Rept.100, June 1966.

[3] Cooke, D.L., "A Self-Consistent Computer Model For The Solar Power Satellite-Plasma Interaction", Ph.D. Thesis for Rice University, Huston TX, May 1981.

[4] Parker, L.W., "Computer Solutions in Electrostatic Probe Theory", Mt.Auburn Research Associates, Inc., Newton MA, AFAL-TR-72-222, Apr. 1973.

[5] Goldstein, H., Classical Mechanics, Addison-Wesley Publishing Company, Inc., Reading MA, 1950.

Figure 1: Parker, L.W., "Theory of Electron Emission Effects in Symmetric Probe and Spacecraft Sheaths", Lee W. Parker, Inc., Concord MA, AFGL-TR-76-0294, Sept.1976, p.27.

Figure 2: Parker, L.W., "Theory of Electron Emission Effects in Symmetric Probe and Spacecraft Sheaths", Lee W. Parker, Inc., Concord MA, AFGL-TR-76-0294, Sept.1976, p.31.